Title

CROSSED BEAMS PRODUCT ANGULAR DISTRIBUTIONS: MCl AND MI FROM Ba, Sr, Ca, AND Mg + ICl AND BaCN AND BaBr FROM Ba + BrCN

Authors

Mims, Charles A.
Lin, Shen-Maw
Hera, Ronald R.

Publication Date

1972-10-01

LBL-1134
Preprint

CROSSED BEAMS PRODUCT ANGULAR DISTRIBUTIONS: MC1 AND MI FROM Ba, Sr, Ca, AND Mg + IC1 AND BaCN AND BaBr FROM Ba + BrCN

Charles A. Mims, Shen-Maw Lin, and Ronald R. Herm

October 1972

Prepared for the U.S. Atomic Energy Commission under Contract W-7405-ENG-48

LBL-1134

DISCLAIMER

LBL-1134

CROSSED BEAMS PRODUCT ANGULAR DISTRIBUTIONS: MCl AND MI FROM Ba, Sr, Ca, AND Mg + ICl AND BaCN AND BaBr FROM Ba + BrCN

Charles A. Mims*, Shen-Maw Lin†, and Ronald R. Herm

Inorganic Material Research Division,
Lawrence Berkeley Laboratory
and Department of Chemistry,
University of California,
Berkeley, California 94720

ABSTRACT

Primitive product angular distributions of MCl and MI from Ba, Sr, Ca, and Mg + ICl and of BaCN and BaBr from Ba + BrCN have been measured in a crossed beams apparatus employing an electron bombardment ionizer-massfilter detector unit. Product center-of-mass (CM) recoil angle and energy distributions have been fit to the measured laboratory (LAB)

---

*Present address: Department of Chemistry, Massachusetts Institute of Technology, Cambridge, Massachusetts.

†Present address: Department of Theoretical Chemistry, Cambridge University, Cambridge, CB2 1EW, England.

angular distributions by averaging the CM → LAB transformations over the (non-thermal) beam speed distributions. Both the MCl and MI CM product distributions from M + ICl are relatively insensitive to the identity of the attacking atom, except that practically no MgI is formed in the Mg reaction. Other product yield ratios are estimated as ∿2:1 for MCl:MI from ICl, ∿10:1 for BaCN:BaBr from BrCN. All of the reactions favor forward CM product scattering (i.e., MX scattered within 90° of the direction defined by the incident M), although the preference is especially weak in the Ba + BrCN → BaBr + CN reaction. For the ICl reactions, MI are formed with broader CM cross sections and higher average product recoil energies, E', than are MCl; average E' values are ∿8-12 kcal/mole for MI + Cl and ∿3-5 kcal/mole for MCl + I. The results are compared with the features of the analogous alkali atom reactions and are discussed in terms of the likely structures of the intermediates.

Crossed beams studies have determined angular distributions of product scattering from K, Rb, and Cs[1], Na[2], and Li[3] + ICl and from Cs[4] and K[4,5] + BrCN. In general, the results reported for these reactions were quite similar to those found for the reactions of alkali atoms (A) with homonuclear halogen molecules (X_2). The dynamics of these latter reactions have been reationalized in terms of an electron transfer model which pictures the transfer of the valence electron of A to X_2 at a relatively large reactant separation; the reaction then proceeds to form the ionically bound alkali halide product by means of the breakup of the X_2^- intermediate in the force field provided by the A^+ ion. Three groups[6-8] have reported classical trajectory calculations using potential hypersurfaces with the long-range reactant attraction which is suggested by this model. However, the manner in which the intermediate X_2^- decomposes remains uncertain because all three calculations gave results consistent with the experimental findings despite different assumptions regarding the product interactions.

Reference 1 points out that the study of the mixed halogen reactions should help to clarify this uncertainty because the "introduction of asymmetry in the mass distribution

and electronic structure thus provides an opportunity to look for effects which can be related to the dynamics of the breakup of the halogen molecule-ion." Unfortunately, however, the previous crossed beam studies[1-5] with mixed halogens (XY) have provided only limited additional insight into the dynamics of alkali atom reactions because these experiments employed a surface ionization detection technique which failed to distinguish between the AX and AY products. Kinematic analyses[1-3] of the measured laboratory (LAB) angular distributions suggested that ACl is the predominant product of the A + ClI reactions. A triple beam chemiluminescence study[9] provided further support for this conclusion for the K + ClI reaction, although this study did suggest that some KI product was produced as well.

This present paper reports crossed beams measurements of angular distributions for each product channel (MX and MY) of the reactions of Ba, Sr, Ca, and Mg with ClI and of Ba with BrCN. Reactions of halogen molecules with alkaline earth atoms (M) are especially suited to crossed beams studies with an electron bombardment ionizer-massfilter detector unit because the ionization potentials of MF and MCl (and, presumably, MBr and MI as well) are apparently equal to or slightly less than those of M.[10] This suggests that ionization of MX involves the removal of a non-bonding electron situated on the M atom; this is further supported by regularities[11] in the electronic energy states of the MX

molecules. Thus, the potential curves for MX and MX^+ are likely to be quite similar. Consequently, ionization of MX by high energy electron impact should favor production of MX^+; more importantly, the fragmentation ratio, $MX^+:M^+$, should be insensitive to the vibrational excitation in MX. In contrast, studies of the analogous alkali atom reactions by this same technique would be severely hampered by uncertainties regarding the fragmentation patterns of the alkali halides, which may depend sharply on the AX vibrational excitation.[12] However, previous crossed beams studies of Ba + Cl_2[13] and of Ba, Sr, Ca, and Mg + Cl_2 and Br_2[14] have indicated close similarities in the dynamics of reactions of alkali atoms and of the heavier alkaline earth atoms.

EXPERIMENTAL PROCEDURE

The apparatus is the same as that used to study the reactions of Ba, Sr, Ca, and Mg with Cl_2 and Br_2[14]; it is described in detail in Ref. 15. The two beams intersected at a right angle, resulting in a 1-5% attenuation of the M beam and negligible attenuation of the ICl or BrCN (XY) beam. A careful mass scan of the ICl beam indicated that any impurities (e.g., Cl_2 or I_2) were less than 1% abundant. The number density probability speed distributions of both beams were non-thermal and were well-fit by the empirical expression

$$\rho_i(v_i) = N_i(v_i - a_i)^2 \exp\{-(v_i - a_i)^2/\alpha_i^2\}u(v_i - a_i). \quad (1)$$

Here, subscripts 1 and 2 denote the M and XY beams respectively; u(t) is the unit step function (u(t)=0 for $t \leq 0$; u(t)=1 for $t>0$); α_i and a_i are parameters which depend on the beam source temperature and pressure[15a]; and $N_i = 4\pi^{-1/2}\alpha_i^{-3}$. Table I lists the beam operating conditions and Fig. 1 shows the angular profiles of the beams. All data analyses presented in this paper are arrived at by averaging over the actual beam speed distributions (Eq. (1) and Table I). Auxiliary calculations assuming thermal beam speed distributions indicated that the derived center-of-mass (CM) cross section results could be considerably in error if the true halogen beam speed distributions had not been used; on the other hand, recognition of the smaller deviations from thermal behavior of the alkaline earth beams was of less significance.

The LAB scattering angle, Θ, is defined as 0° for the M beam direction and 90° for the XY beam direction. The detector could be rotated about the beam intersection volume, in the plane defined by the two beams, so as to scan a range of Θ from -15° to +115°. The detector angular resolution response function was similar in shape to the M beam angular profile shown in Fig. 1. No measurements of the product LAB speed were made; only product LAB angular distributions are reported here. The neutral products were ionized by electron

bombardment (at ∿150 e.v.) and detected, after mass analysis, via electron multiplier amplification. All product angular distributions were measured with the massfilter set at the MX^+ or MY^+ peak. Careful mass scans for several of the scattering partners (Ba and Mg + ClI and Ba + BrCN) failed to disclose any MXY^+ scattered signal.

DATA ANALYSIS AND RESULTS

The data analysis procedure, described in more detail in Refs. 14 and 15, consists in assuming a form for the CM cross section, $\sigma(\theta,u)$, and calculating the resultant LAB product number density angular distribution by averaging over the beam speed distributions and integrating over the unmeasured LAB speed of the detected product, v:

$$I_{LAB}(\theta) = \int_0^{v^*}\int_0^{\infty}\int_0^{\infty} V\sigma(\theta,u)(v/u^2)\rho_1(v_1)\rho_2(v_2)dv_1dv_2dv. \quad (2)$$

In the CM coordinate system, θ and u are the recoil angle and speed of the detected product; θ is defined as 0° (forward scattering) where $\vec{u}$ lies along the initial relative velocity vector, $\vec{V}$, in the direction defined by the M atom. The calculated LAB angular distribution is compared with the measured data, and the procedure is repeated until, by trial and error, a form of $\sigma(\theta,u)$ is obtained which provides a good fit to the data.

The integration over v shown in Eq. (2) is limited to a finite range (0 to v^*) determined by the reaction energetics. For the M + XY → MX + Y reaction, where the MX product is detected, the energy with which the MX and Y products recoil apart, E', and the internal excitations of MX and Y, W', are related to the initial XY internal excitation, W, and the reactant relative collision energy, $E = (m_M m_{XY}/2m_{MXY})v^2$, by

$$E' + W' = E + W + \Delta D_o, \tag{3}$$

where

$$\Delta D_o = D_o(MX) - D_o(XY), \tag{4}$$

$$E' = (m_{MXY} m_{MX}/2m_Y)u^2, \tag{5}$$

and the m's denote the masses of the particles. Table II lists values of E, W, and ΔD_o; v^* was calculated for each reaction by setting E = W = W' = 0. Although $D_o(Cl - I)$[16], $D_o(Br - CN)$[16], and $D_o(M - Cl)$[10b] are well known, there are no reliable experimental determinations of the bond energies of MBr, MI, or MCN. The values used here for MI and MBr are from an ionic bonding model calculation.[17] The value used for BaCN is an estimate[15a] which is based on an empirical correlation[18] between the energy required for separation into ions and the bond lengths in the alkali halides. Moreover, the true structure of this product might be BaCN or BaNC; Hartree-Fock calculations reported in Ref. 19 indicate that LiNC is marginally more stable than LiCN.

Although the data could undoubtedly be fit by more complicated CM cross section functions, all of the derived CM cross sections which are presented here are of the simple form:

$$\sigma(\theta,u) = T(\theta)U(u). \tag{6}$$

In some of the data analyses, it has further proven convenient to express $T(\theta)$ and $U(u)$ as:

$$T(\theta) = (1 - C_1)\exp\{-\ell n2(\theta/H_1)^2\} + C_1, \text{ and} \tag{7a}$$

$$U(u) = (u/u_1)^{n_1}\exp\{(n_1/m_1)(1 - (u/u_1)^{m_1})\}, \; u \leq u_1, \tag{7b}$$

$$U(u) = (u/u_1)^{n_2}\exp\{(n_2/m_2)(1 - (u/u_1)^{m_2})\}, \; u \geq u_1,$$

where all subscripted variables serve as adjustable parameters. Owing to its limited information content, a number of $T(\theta)$ - $U(u)$ combinations will often fit the primitive (i.e., no product velocity analysis) LAB angular distributions which are reported here. In order to provide insight into the range of CM cross sections which are compatible with the experimental data, at least two data analyses are presented for each reaction. One of these, termed the "Single Recoil Energy" (SRE) result, assumes that the products separate with a single, fixed product recoil energy (i.e., $U(u)$ is approximated as a delta function). Because the full breadth of the measured LAB angular distribution must be accounted for by the $T(\theta)$

function, the SRE result should provide an upper limit on the overall breadth of the peak in the true CM angular distribution. The opposite data analysis extreme presented, termed the "Narrow Angular Distribution" (NAD) result, seeks the $T(\theta)$ function, given by Eq. (7a), with the narrowest breadth about its peak which can be fit to the data; this extreme should provide an upper limit for the dispersion in the recoil speed distribution.

$$M + ClI \rightarrow MCl + I$$

Figure 1 shows that the measured LAB MCl^+ signals all peak at considerably smaller Θ values than do the calculated angular distributions (assuming an energy independent collision cross section) of the LAB velocity of the center-of-mass of the collision partners, $\vec{C}$; furthermore, the data points fall off smoothly with angle through the angular regions of the peaks of the $\vec{C}$ distributions. These comparisons show that the MCl^+ measured signals must have arisen from ionization of an MCl product which had scattered predominately into the forward CM hemisphere. Figure 1 also shows the fits to the measured data which are provided by the SRE and NAD CM recoil functions given in Fig. 2 and Table III; $P(E')$ was calculated from $U(u)$, by means of Eq. (5), as $P(E')dE' = U(u)du$.

Calculations for a variety of other CM cross sections have also indicated the following properties of all of the MCl angular distributions: (1) any $T(\theta)$ symmetric about 90°

is incompatible with the data; (2) $T(\theta)$ must peak within $\theta \lesssim 20°$; (3) $T(\theta)$ might actually have a secondary peak at 180°, but it cannot be more than ~20-25% of the forward peak; and (4) $T(\theta)$ cannot be broader than the SRE fit, nor much narrower than the NAD fit. Furthermore, as is pointed out in Ref. 14, the true CM cross sections should be much closer to the NAD results than to the SRE results because of the unrealistic treatment of the recoil energy distribution in the SRE procedure and because the NAD results are qualitatively similar in shape to product velocity analysis results for some reactions of alkali atoms with halogen molecules.

Table III also includes values for the fraction of the products, Q_F, which is scattered into the forward CM hemisphere:

$$Q_F = \int_0^{\pi/2} T(\theta) \sin\theta d\theta \Big/ \int_0^{\pi} T(\theta) \sin\theta d\theta. \qquad (8)$$

These indicate a tendency for Mg to produce less MCl forward scattering than do the other alkaline earth atoms. The characteristic E' values given in Table III, together with the ΔD_o entries of Table II, also clearly indicate that most of the reaction exothermicities appear as internal excitations of the products.

$$M + ICl \rightarrow MI + Cl$$

Figures 3 and 4 show that the measured BaI^+, SrI^+, and CaI^+ signals peak at smaller LAB angles than do the calculated distributions of $\vec{C}$, again indicating that the MI products are scattered predominately into the forward CM hemisphere. Furthermore, the smooth decrease with angle through the angular regions of the peaks in the $\vec{C}$ distributions which are apparent in the MCl^+ and MI^+ distributions in Figs. 1, 3, and 4 clearly indicate that little (if any) of the measured product signal arises from ionization of an MICl complex which would necessary recoil in the LAB along $\vec{C}$.

The LAB↔CM transformation diagram for the Ba + ICl → BaI + Cl reaction which is included in Fig. 3 illustrates that the observation of appreciable product intensity at small and even negative LAB angles, as is shown in Figs. 3 and 4, requires an appreciable product recoil energy for a significant fraction of the reactions. Furthermore, this transformation diagram, as well as Eq. (5), illustrates that the large m_{MI}/m_{Cl} product mass ratio restricts the MI product CM recoil speed to relatively small values even for rather large values of E'. Owing to the rather wide angular distribution of $\vec{C}$, this in turn makes the measured MI LAB angular distribution much less sensitive than the MCl LAB distribution to the form of the CM cross section.

This insensitivity is reflected in the wide range of CM fits to the data which are presented in Figs. 3 and 4 and Table III. Although the NAD (denoted "C" in Table III) cross

sections do provide fits to the measured M + ICl data, they are unlikely to reflect the true shapes of the CM cross sections for two reasons: (1) the NAD fits to the Sr and Ca + ICl reactions were obtained only by assuming the very upper extremes for the ΔD_o values given in Table II; and (2) a very specialized and unrealistic reaction mechanism would likely be required to account for a very sharply forward directed product angular distribution while, at the same time, providing such a large dispersion in the product recoil energy distribution. Since the SRE fit makes a very restrictive assumption regarding the form of P(E'), the true CM cross sections are likely to fall somewhere within the range of the A and B fits of Figs. 3 and 4 and Table III. Here again, calculations for a variety of other CM cross sections also indicate that (1) $T(\theta)$ cannot be symmetric about 90° and (2) $T(\theta)$ favors scattering into the forward CM hemisphere, as illustrated by the Q_F entries in Table III.

Because the detector response may vary each time the apparatus is exposed to atmospheric pressure, it is not possible to extract absolute total reaction cross reactions, Q_T, nor even relative values for reactions of different alkaline earth atoms, although a general trend of decreasing LAB product intensity was noted in going from reaction of Ba to that of Mg. For a fixed alkaline earth atom, data on the MI^+ and MCl^+ angular distributions were collected during the same apparatus pumpdown. Thus, the absolute measured MI^+ and MCl^+

signals may be used to calculate $Q_T(MCl)/Q_T(MI)$ by simply correcting for the ratio (β) of MCl and MI detection efficiencies and integrating the CM cross sections over recoil speed and solid angle. Although β is rather uncertain, Ref. 15a presents arguments which indicate that it is likely to be close to unity. Assuming $\beta = 1$, the different combinations of derived CM cross sections given in Table III provide $Q_T(MCl)/Q_T(MI)$ ratio ranges of 1.3-2.3 for Ba and Sr and 1.5 to 3.2 for Ca. If only the more likely CM cross sections are used (i.e., the NAD MCl results and the A and B MI results), $Q_T(MCl)/Q_T(MI)$ becomes $\sim$1.8 for Ba and Sr and $\sim$2.1 for Ca. A very weak MgI^+ signal from Mg + ICl was also detected; although it proved to be too noisy to permit measurement of an MgI angular distribution, its magnitude suggested that $Q_T(MgCl)/Q_T(MgI) > \sim 5$. The uncertain thermochemistry of these reactions prevents a comparison of these ratios with a statistical theory[20] calculation. However, it is pertinent to note that Ref. 1 gives statistical theory calculations of this ratio as 1.8 for K + ClI and 1.2-1.3 for Cs + ClI.

The Ba + BrCN → BaNC and BaBr Reactions

Fig. 5 shows the measured LAB $BaCN^+$ and $BaBr^+$ signals scattered from Ba + BrCN. Although the $BaBr^+$ signal is not sufficiently distinct from the calculated $\vec{C}$ distribution to preclude the chance that is arose (at least partly) from

ionization of BaBrCN, the data were analyzed assuming BaCN and BaBr products. The BaBr product suffers from the same product mass ratio problem which was encountered with MI. Figure 5 and Table III indicate that a wide range of CM cross sections will fit the data. This is true to a lesser extent with BaCN as well because this data was collected near the end of our studies of alkaline earth atom chemistry; consequently, the detector was dirty, signal-to-noise had deteriorated, and unforeseen factors brought the experiment to a premature end before the wide-angle scattering had been measured. Nevertheless, the data do indicate that BaCN is more sharply scattered forward than is BaBr. The integrated total cross section ratio, $Q_T(BaCN)/Q_T(BaBr)$, is calculated to be $\sim$7-20.

DISCUSSION

Although there is considerable uncertainty in the derived CM cross sections, the data clearly indicate two qualitative differences between the M + ICl → MI + Cl and M + ClI → MCl + I reactions. First, the entries in Table III indicate that the MI and Cl products recoil with appreciably higher average energy than do the MCl and I products; since ΔD_o is less for the M + ICl reaction, this corresponds to an even greater disparity in the fraction of the reaction exothermicity which appears as product recoil. These E' entries also indicate

that the product recoil energy is relatively insensitive to the identity of the attacking alkaline earth atom. The second difference which is apparent between these reactions is that the MI product is scattered with a much broader CM cross section than is the MCl product. Although the data analyses do not unequivocally establish whether this added breadth appears in the recoil angle or energy distribution, the "most likely" analyses suggest that both distributions are broadened for the MI product. Property (2) might be a consequence, at least in part, of property (1), as the enhanced product recoil energy might be expected to broaden the forward peaked product angular distribution.

The features of the scattering of the MCl product which are observed here are similar to those found in the reactions of Cl_2 with alkaline earth[13,14] and alkali[21] atoms and are understandable in terms of the simple one electron transfer model of alkali atom reactions. Details of this model for the A + ICl reaction are given in Ref. 1. These authors point out that the lowest unfilled orbital on ICl, which accepts the alkali valence electron, is likely to be located predominately on the I atom for the Cl-I internuclear separations at which the $ICl \rightarrow ICl^-$ vertical jump takes place. However, in free space, this ground state of ICl^- correlates asymptotically with $I + Cl^-$; of course, for certain configurations, the presence of the A^+ could change this asymptotic correlation to $Cl + I^-$. Nevertheless, Kwei and Herschbach[1]

argue that this effect will favor formation of the MCl product, at least for large impact parameter collisions where pre-migration of the charge in ICl^- is likely to be favored.[22] Thus, the simple one electron transfer model would provide an explanation of the CM product angular distributions which are observed here because it suggests that MCl rather than MI is likely to be formed in the large impact parameter collisions which should favor forward scattering. The MI (and possibly some MCl) would be formed in smaller impact parameter collisions which would tend to produce a broader product angular distribution.

However, the relatively large MI + Cl product recoil energies and the contrast between those of MI + Cl and MCl +I which are reported here are not currently adequately explained by this one electron transfer model and the existing classical trajectory calculations[6-8] on potential surfaces suggested by this model. The observations are probably best reconciled with the model by postulating that the MI + Cl scattering observed here represents a special subset, which might favor certain particular initial conditions, of the total reactive events. This would then be consistent with existing information on the A + X_2 reactions because: (1) trajectory calculations[6-8] as well as product velocity analysis measurements[23] indicate that, although small product recoil energies are favored, a substantial fraction of the reactions actually lead to appreciable product recoil energies; and (2) the

trajectory calculations[8b] do indicate a possible correlation between initial trajectory conditions and the partitioning of the reaction energy.

An alternate possibility is that the M + ICl reactions studied here are not really analogous to the A + ICl reactions because of the stability of MICl and the resultant deep chemical well in the potential hypersurface for the M + ICl reactions. Since the bonding in the heavier-alkaline-earth dihalides is probably largely ionic,[10] reactive trajectories which sample this well might be said to undergo a "two electron transfer" mechanism, corresponding to the reaction sequence: $M + XY \rightarrow M^{+} \ldots XY^{-} \rightarrow X^{-} \ldots M^{+2} \ldots Y^{-} \rightarrow M^{+}X^{-} + Y$. Previous studies[13,14] which noted the similarities between the reactions of M and A with Cl_2 and Br_2 indicated that this deep well in the potential surface did not dominate the dynamics of these reactions of the alkaline earth atoms; however, these studies would probably have been insensitive to the influence of the well in as many as 20-30% of the reaction trajectories. Moreover, the electronic asymmetry of ICl removes the symmetry restriction on broadside attack along the C_2 axis which might influence the M + X_2 reactions.[14] Thus, the data presented here might be explained by postulating that some of the reactive trajectories proceed via an alkali-like one electron trasfer to form (predominately) MCl (or BaCN). However, a substantial fraction of the trajectories would follow the two electron transfer mechanism. It is quite conceivable

that an $Cl^{-}M^{+2}I^{-}$ complex, which would be very highly internally excited, might dissociate into MI and Cl with a high recoil energy and in a time which was shorter than or comparable to its rotational period so as to be consistent with the observed asymmetry of the product angular distributions. This might happen via a direct mechanism which could even favor formation of MI over MCl because of the greater mobility of the Cl atom. Alternatively, such a complex might tend to distribute the reaction energy statistically, which would again lead to relatively high E' values; in this case, however, decomposition into both product channels would be expected. Indeed, this is consistent with the data as well because the detector is most sensitive to products scattered in the CM system along $\theta = 0°$ (or 180°) with small E' values. Calculations reported in Ref. 15a indicate that an MCl component scattered with the absolute $\sigma(\theta,E')$ observed for the MI product would appear in the LAB as only a small (i.e., $\sim$10-30%) addition to the contribution from the CM cross sections given in Fig. 2 and Table III. These possibilities point out the need for product velocity analysis measurements on the reactions studied here as well as further trajectory calculations on potential surfaces which attempt to simulate the asymmetries introduced by the mixed halogens.

ACKNOWLEDGMENTS

This work was supported by the Atomic Energy Commission through the Lawrence Berkeley Laboratory. Partial support from the Committee on Research of the University of California at Berkeley is also gratefully acknowledged.

REFERENCES

1. G.H. Kwei and D.R. Herschbach, J. Chem. Phys. 51, 1742 (1969).
2. J.H. Birely, E.A. Entemann, R.R. Herm, and K.R. Wilson, J. Chem. Phys. 51, 5461 (1969).
3. D.D. Parrish and R.R. Herm, J. Chem. Phys. 51, 5467 (1969).
4. R. Grice, M.R. Cosandey, and D.R. Herschbach, Ber. Bunsenges. Phys. Chem. 72, 975 (1968).
5. J.C. Whitehead, D.R. Hardin, and R. Grice, Mol. Phys. 23, 787 (1972).
6. N.C. Blais, J. Chem. Phys. 49, 9 (1968); 51, 856 (1969).
7. M. Godfrey and M. Karplus, J. Chem. Phys. 49, 3602 (1968).
8. (a) P.J. Kuntz, E.M. Nemeth, and J.C. Polanyi, J. Chem. Phys. 50, 4607 (1969); (b) P.J. Kuntz, M.H. Mok, and J.C. Polanyi, J. Chem. Phys. 50, 4623 (1969).
9. M.C. Moulton and D.R. Herschbach, J. Chem. Phys. 44, 3010 (1966).
10. (a) D.L. Hildebrand, J. Chem. Phys. 48, 3657 (1968); (b) 52, 5751 (1970).
11. W.H. Hamill, J. Chem. Phys. 56, 4191 (1972).
12. H.J. Loesch and D.R. Herschbach, J. Chem. Phys. 57, 2038 (1972).
13. J.A. Haberman, K.G. Anlauf, R.B. Bernstein, and F.J. Van Itallie, Chem. Phys. Letters (to be published).

14. S.-M. Lin, C.A. Mims, and R.R. Herm, to be published.

15. (a) C.A. Mims, Ph.D. thesis, University of California, Berkeley, 1972; (b) S.-M. Lin, Ph.D. thesis, University of California, Berkeley, 1972.

16. B. deB. Darwent, Bond Dissociation Energies in Simple Molecules, Nat. Stand. Ref. Data Ser., Nat. Bur. Stand. (U.S.), NSRDS-NBS 31 (1970).

17. K.S. Krasnov and N.V. Karaseva, Opt. Spectrosc. 19, 14 (1965).

18. R.R. Herm and D.R. Herschbach, J. Chem. Phys. 52, 5783 (1970).

19. B. Bak, E. Clementi, and R.N. Kortzeborn, J. Chem. Phys. 52, 764 (1970).

20. J.C. Light, Disc. Faraday Soc. 44, 14 (1967).

21. A recent review of crossed beam kinetics studies is given in: J.L. Kinsey, MPT International Review of Science, edited by J.C. Polanyi (Butterworths, London, 1972), Physical Chemistry Series One, Vol. 9, Chap. 6.

22. Further evidence for the influence of the asymmetry of the ICl electronic structure on reaction dynamics is also provided (for a much different dynamical range) by crossed beams studies of the reactions of D atoms with ICl reported in: J.D. McDonald, P.R. Le Breton, Y.T. Lee, and D.R. Herschbach, J. Chem. Phys. 56, 769 (1972).

23. K.T. Gillen, A.M. Rulis, and R.B. Bernstein, J. Chem. Phys. 54, 2831 (1971) and references cited therein.

Table I. Experimental beam conditions[a]

reaction	Alkaline earth atom beam				Halogen beam			
	source conditions		speed distribution[b,c]		source conditions		speed distribution[b,d]	
	temperature	pressure	α_1	a_1	temperature	pressure	α_1	a_1
Ba + ClI	1000	0.14	3.3	0.6	350	2.4	1.9	1.5
Ba + ICl	1010	0.15	3.3	0.6	340	2.8	1.9	1.5
Sr + ClI	980	0.6	3.8	1.3	340	3.0	1.9	1.5
Sr + ICl	980	0.6	3.8	1.3	340	2.7	1.9	1.5
Ca + ClI	1040	0.6	5.8	1.9	360	2.3	1.9	1.5
Ca + ICl	1060	0.7	5.9	1.9	360	2.3	1.9	1.5
Mg + ClI	860	0.8	6.8	2.2	350	3.0	1.9	1.5
Ba + NCBr	1080	0.6	3.2	1.1	350	2.7	2.3	1.9
Ba + BrCN	1120	1.0	3.3	1.1	350	2.6	2.3	1.9

[a]Temperatures are given in °K, pressures in torr, and speeds in 100 m/sec. Data are given for the M + XY → MX + Y reaction.

[b]Symbols refer to parameters of Eq. (1).

[c]Parameters for Ba are based on actual measurements; parameters for Sr, Ca, and Mg are from an extrapolation discussed in Ref. 15a.

[d]Parameters for ICl are based on actual measurements; parameters for BrCN are from an extrapolation discussed in Ref. 15a.

Table II. M + XY → MX + Y reaction energetics[a]

reaction	relative collision energy, E[b]	reactant internal excitation, W[c]	reaction exoergicity, ΔD_o
Ba + ClI	2.1	1.0	55 ± 3
Ba + ICl	2.1	1.0	35 ± 15
Sr + ClI	2.7	1.0	46 ± 3
Sr + ICl	2.7	1.0	30 ± 15
Ca + ClI	2.9	1.0	45 ± 3
Ca + ICl	2.9	1.0	25 ± 15
Mg + ClI	2.5	1.0	25 ± 3
Mg + ICl	-	-	5 ± 10
Ba + NCBr	2.6	1.5	30[d]
Ba + BrCN	2.6	1.5	10 ± 15

[a]All energies are given in kcal/mole.

[b]Calculated for the most probable (number density distributions) beam speeds.

[c]The average thermal rotational and vibration energy in XY which is given here would be too large if the internal degrees of freedom relaxed in the beam expansion process.

[d]This is an estimate.

Table III. M + XY → MX + Y derived CM reaction cross sections[a]

reaction	legend	angular distribution[b]			speed distribution[c]		recoil energy[d]	
		H_1	C_1	Q_F	u_1	n_1,m_1,n_2,m_2	$\bar{E}'$	$\langle E' \rangle$
Ba + ClI	SRE	-	-	0.72	-	-	3.3	3.3
	NAD	16	0.08	0.62	3.2	3,2,2,3	3.3	4.7
Sr + ClI	SRE	-	-	0.70	-	-	3.3	3.3
	NAD	20	0.10	0.67	4.5	3,2,2,3	3.9	5.4
Ca + ClI	SRE	-	-	0.72	-	-	2.8	2.8
	NAD	20	0.09	0.65	6.0	3,2,2,3	3.5	4.9
Mg + ClI	SRE	-	-	0.61	-	-	2.8	2.8
	NAD	15	0.15	0.56	8.0	2,1,2,2	1.7	5.3
Ba + ICl	SRE	-	-	0.58	-	-	9.0	9.0
	A	135	0.00	0.60	2.2	10,2,2,10	11.7	11.5
	B	-	-	0.60	2.5	3,2,2,3	11.1	13.8
	C	15	0.17	0.55	2.7	2,1,2,2	4.9	11.6
Sr + ICl	SRE	-	-	0.62	-	-	8.0	8.0
	A	120	0.00	0.63	2.5	10,2,2,10	11.1	10.9
	B	-	-	0.60	3.0	3,2,2,3	10.8	11.1
	C	15	0.17	0.55	3.5	2,1,2,2	5.5	11.1
Ca + ICl	SRE	-	-	0.61	-	-	8.0	8.0
	A	120	0.00	0.63	3.1	10,2,2,10	9.9	9.7
	B	-	-	0.60	4.0	3,2,2,3	12.2	10.4
	C	15	0.17	0.55	4.0	2,1,2,2	4.6	11.5

Table III. (continued)

Ba + NCBr	SRE	-	-	0.67	-	-	2.8	2.8
	NAD	10	0.07	0.56	3.2	2,1,2,2	1.4	5.1
Ba + BrCN	SRE	-	-	0.52	-	-	4.0	4.0
	NAD	15	0.30	0.53	2.0	2,1,2,2	2.4	4.4

[a]Energies are given in kcal/mole, speeds in 100 m/sec, and angles in degrees.

[b]H_1 and C_1 are parameters of Eq. (7a) and Q_F is the fraction scattered forward (Eq. (8)). If no entries are given for H_1 and C_1, $T(\theta)$ was not restricted to the form of Eq. (7a).

[c]These are the parameters of Eq. (7b).

[d]$dP(E')/dE'\big|_{E'=\bar{E}'} = 0$; $\langle E' \rangle = \int_0^{\Delta D_o} E'P(E')dE' \Big/ \int_0^{\Delta D_o} P(E')dE'$. All fits refer to ΔD_o values given in Table II except the C fits for Ca and Sr + ICl. These provided fits only if ΔD_o was assumed to be the upper limit given in Table II.

FIGURE CAPTIONS

Fig. 1. The data points show the measured LAB angular distributions of MCl^+ signal for scattering of Mg, Ca, Sr, and Ba from ClI; different data symbols indicate results obtained on different apparatus pumpdowns. The dotted curves show the calculated angular distributions of the LAB velocity of the center-of-mass, $\vec{c}$. The dashed and solid curves show the SRE and NAD fits, respectively, to the data provided by CM cross sections given in Fig. 2 and Table III. Also shown are angular profiles of the two beams.

Fig. 2. The SRE (dashed) and NAD (solid) CM angular distributions of MCl product which provide the fits to the LAB data shown in Fig. 1. The corresponding CM MCl recoil speed distributions are given in Table III; the corresponding product recoil energy distribution, P(E'), is shown here for Ba + ClI.

Fig. 3. Measured LAB BaI^+ scattered signal from Ba + ICl; different data symbols were collected on different apparatus pumpdowns. The two lower panels show different derived CM angle and recoil energy distributions; parameters for these functions are listed in Table III; the SRE (dashed) $T(\theta)$ functions peaking at 0° and at 30° provide the same fit to the LAB data. The top panel shows the SRE, A, and C

fits to the data; the B fit (not shown) is as good. Also shown are a calculated distribution in $\vec{C}$ (dotted curve) and a LAB↔CM transformation diagram; the circles show loci of BaI CM recoil speeds for some possible product recoil energies, E' (kcal/mole).

Fig. 4. Measured MI^+ LAB signals scattered from Sr and Ca + ICl and derived MI CM product angular distributions; the corresponding CM MI recoil speed distributions are given in Table III. The B and C fits to the LAB data (not shown) are as good as the SRE and A fits which are shown. Other conventions are as described in Fig. 3.

Fig. 5. The data points show the measured LAB $BaCN^+$ and $BaBr^+$ signals scattered from Ba + BrCN. Also shown are the derived SRE (dashed) and NAD (solid) BaCN and BaBr CM Product angular distributions (recoil speed distribution parameters given in Table III) which provide the indicated fits to the data. Dotted curves show the calculated distributions in $\vec{C}$.

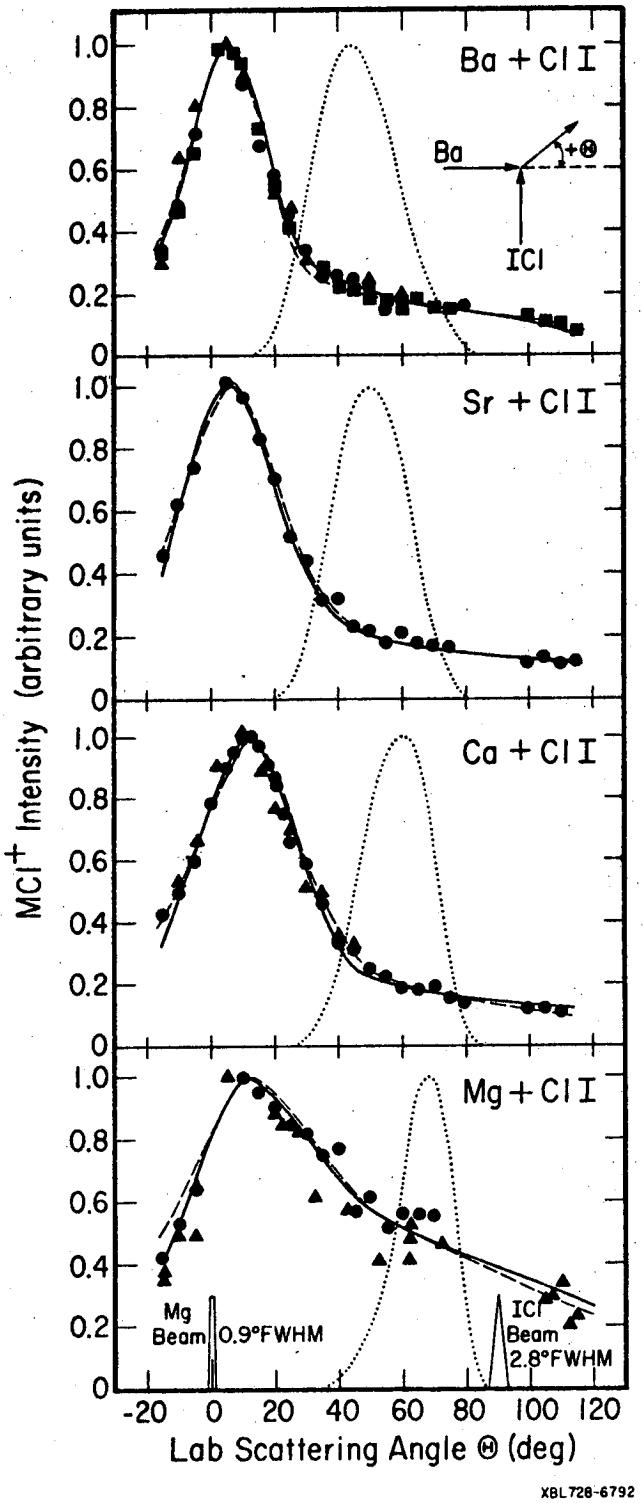

Fig. 1.

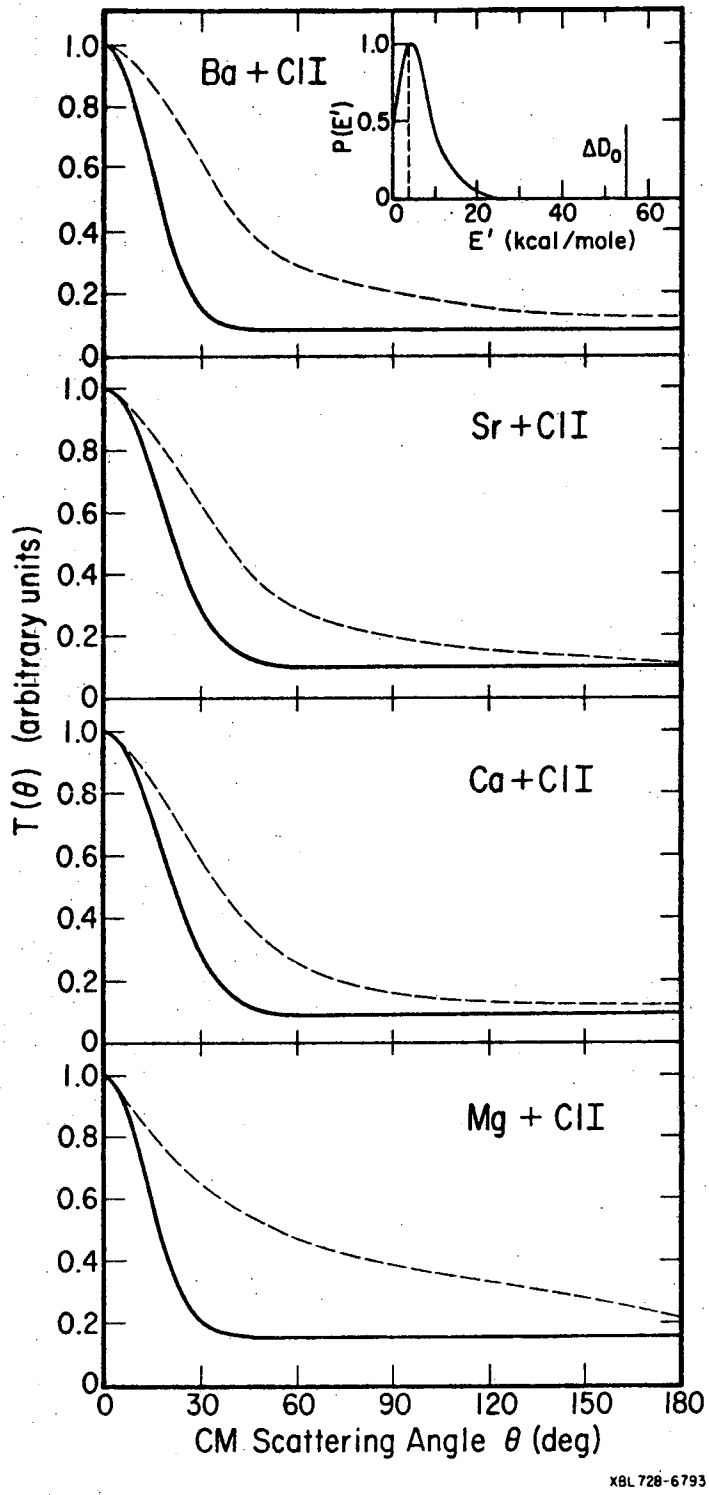
Ba + ClI
Sr + ClI
Ca + ClI
Mg + ClI
P(E')
ΔD0
E' (kcal/mole)
T(θ) (arbitrary units)
CM Scattering Angle θ (deg)
X8L 728-6793

Fig. 2.

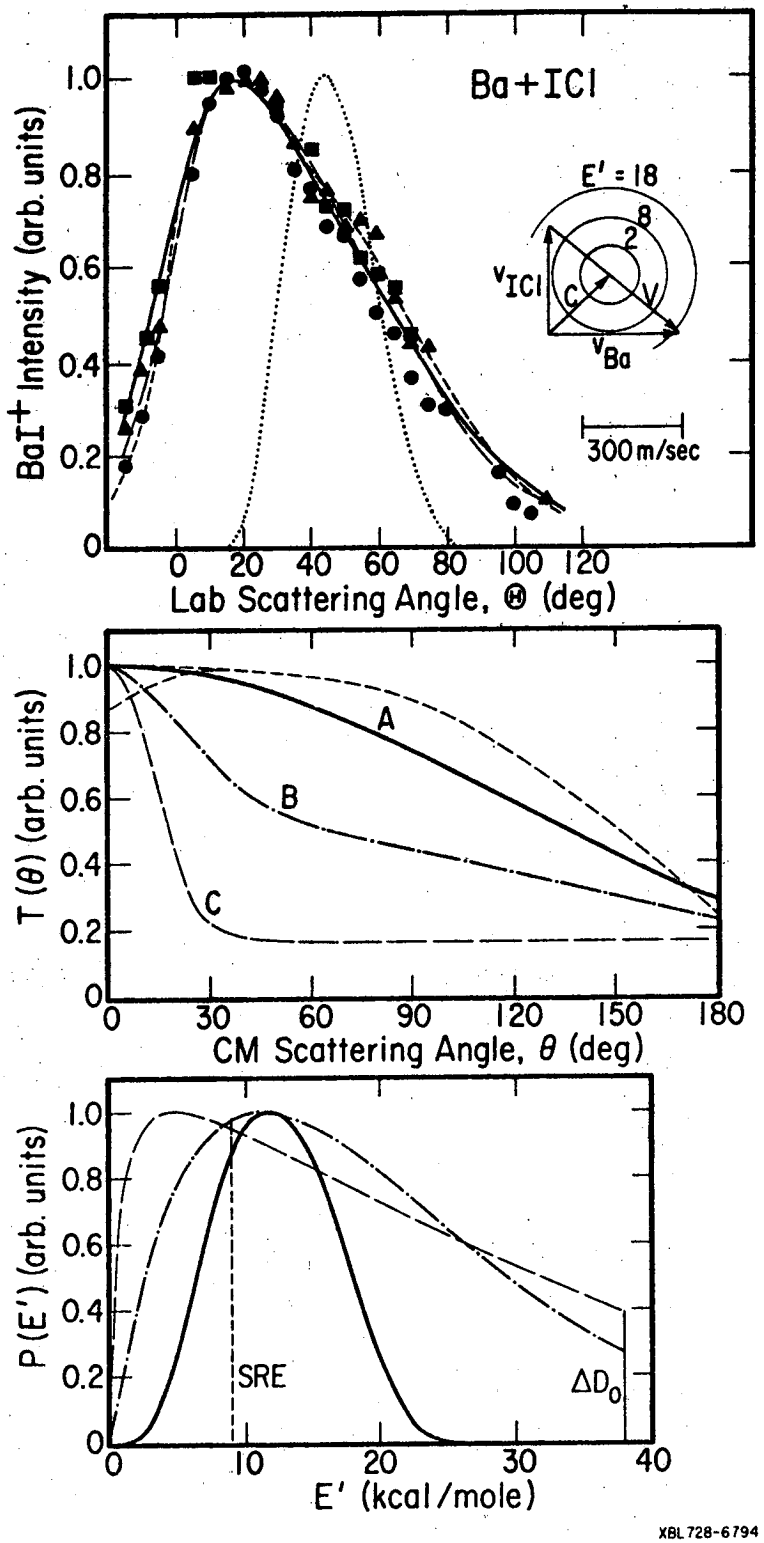
Ba+ICl
E' = 18
8
2
v_{ICl}
C
V
v_{Ba}
300 m/sec
BaI^+ Intensity (arb. units)
Lab Scattering Angle, Θ (deg)
T (θ) (arb. units)
A
B
C
CM Scattering Angle, θ (deg)
P(E') (arb. units)
SRE
ΔD_0
E' (kcal/mole)
XBL728-6794

Fig. 3.

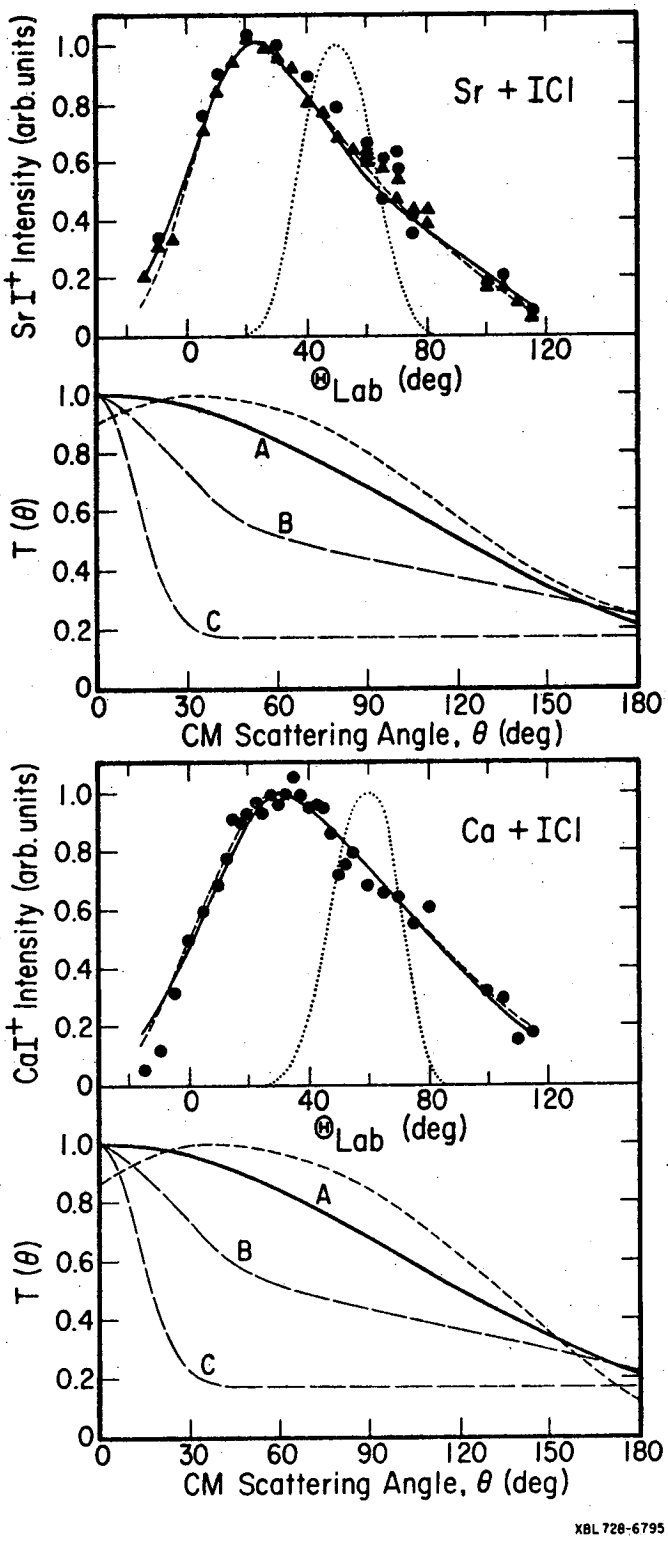
Sr + ICl
SrI+ Intensity (arb. units)
Θ Lab (deg)
T (θ)
A
B
C
CM Scattering Angle, θ (deg)
Ca + ICl
CaI+ Intensity (arb. units)
Θ Lab (deg)
T (θ)
A
B
C
CM Scattering Angle, θ (deg)
XBL 728-6795

Fig. 4.

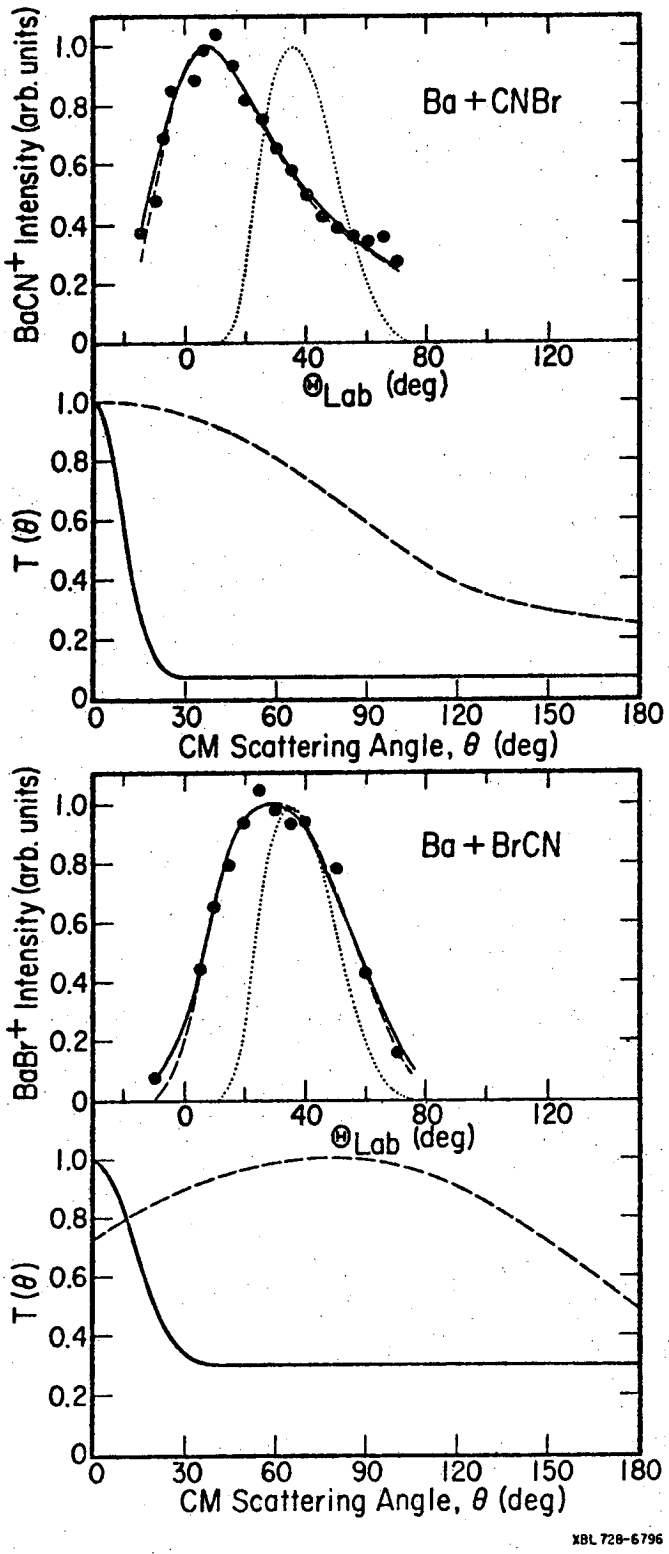
Ba + CNBr
BaCN+ Intensity (arb. units)
1.0
0.8
0.6
0.4
0.2
0
0
40
80
120
ΘLab (deg)
T (θ)
1.0
0.8
0.6
0.4
0.2
0
0
30
60
90
120
150
180
CM Scattering Angle, θ (deg)
Ba + BrCN
BaBr+ Intensity (arb. units)
1.0
0.8
0.6
0.4
0.2
0
0
40
80
120
ΘLab (deg)
T (θ)
1.0
0.8
0.6
0.4
0.2
0
0
30
60
90
120
150
180
CM Scattering Angle, θ (deg)
XBL 728-6796

Fig. 5.

TECHNICAL INFORMATION DIVISION
LAWRENCE BERKELEY LABORATORY
UNIVERSITY OF CALIFORNIA
BERKELEY, CALIFORNIA 94720